

PRECISION VALIDATION OF MIPAS-ENVISAT PRODUCTS

Chiara Piccolo and Anu Dudhia

*Atmospheric, Oceanic & Planetary Physics, University of Oxford, Parks Rd, Oxford OX1 3PU, UK
Email: dudhia@atm.ox.ac.uk*

ABSTRACT

This paper discusses the variation and validation of the precision (defined as the dispersion of an ensemble of retrievals obtained from measurements of the same atmospheric state) of the ESA L2 products from the Michelson Interferometer for Passive Atmospheric Sounding (MIPAS).

The MIPAS L2 products contain estimates of random error derived from the propagation of the radiometric noise through the retrieval. The noise itself varies with time, steadily rising between decontamination events, but its contribution to the L2 random error also depends on the atmospheric temperature, which controls the total radiance received. Hence, for all species, the random error varies latitudinally/seasonally with atmospheric temperature, with a superimposed time dependence on decontamination events.

The precision validation involves comparing two MIPAS retrievals at the intersections of ascending/descending orbits. For every 5 days per month of high resolution MIPAS operation, the standard deviation of the statistic of the matching profile pairs is computed and compared with the predicted random error given in the MIPAS Offline L2 data. Even taking into account the propagation of the pressure-temperature retrieval errors into the VMR retrieval, the observed scatter is usually a factor 1-2 larger than the predicted error. This is thought to be due to effects such as horizontal inhomogeneity of the atmosphere.

Key words: MIPAS, precision, random error.

1. INTRODUCTION

The Michelson Interferometer for Passive Atmospheric Sounding (MIPAS) is an infrared limb-sounding Fourier transform interferometer on board the Envisat satellite, launched in March 2002 [1, 2]. It acquires spectra over the range $685 - 2410 \text{ cm}^{-1}$ ($14.5 - 4.1 \mu\text{m}$), which includes the vibration-rotation bands of many molecules of interest. It is capable of measuring continuously around

an orbit in both day and night and a complete global coverage is obtained in 24 hours.

From July 2002 until March 2004 MIPAS was operated at full spectral resolution (0.025 cm^{-1}) with a nominal limb-scanning sequence of 17 steps from $68 - 6 \text{ km}$ with 3 km tangent height spacing in the troposphere and stratosphere, generating complete profiles spaced approximately every 500 km along the orbit. However, in March 2004 operations were suspended following problems with the interferometer slide mechanism. Operations were resumed in January 2005 with a 35% duty cycle and reduced spectral resolution (0.0625 cm^{-1}).

For the high-resolution mission ESA have processed pT (pressure-temperature) and 6 “key species” (H_2O , O_3 , HNO_3 , CH_4 , N_2O and NO_2). The algorithm used for the Level 2 analysis is based on the Optimised Retrieval Model (ORM) [3, 4].

This paper presents the validation of the precision of the vertical profiles of ESA L2 Offline MIPAS data for the period July 2002 – March 2004 when the instrument was operating at full resolution.

2. PREDICTED RANDOM ERROR

The main source of the random error of the ESA L2 Offline MIPAS profiles is the noise error due to the mapping of the radiometric noise in the retrieved profiles. This predicted random error is proportional to the NESR (Noise Equivalent Spectral Radiance) and inversely proportional to the Planck function (therefore atmospheric temperature), but it does not directly depend on the VMR of the gases.

In the ESA retrieval processing, first, temperature and tangent pressure are retrieved simultaneously, then the 6 “key species” VMR profiles are retrieved individually in sequence. The effects of temperature and pressure errors on the VMR retrievals are taken into account in the predicted random error estimation.

The predicted random error given in the MIPAS Offline L2 data has been averaged for every 5 days per month of high resolution MIPAS operation. Figs. 1 and 2 show an

example of the time series of the predicted random error for H_2O and HNO_3 , respectively.

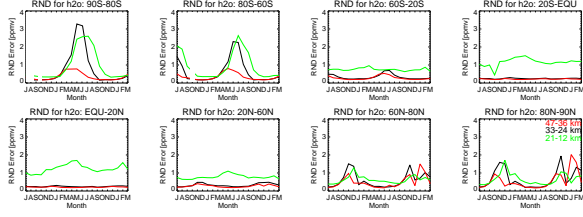


Figure 1. Time series of the random error derived from MIPAS Offline L2 data for H_2O [ppmv] from July 2002 to March 2004, split in eight latitude bands. The red line shows the random error averaged between 47 km and 36 km tangent heights, the black line between 33 km and 24 km and the green line between 21 km and 12 km. The gaps in the southern hemisphere in July-August 2002 and October 2002 are caused by missing Antarctic L2 profiles.

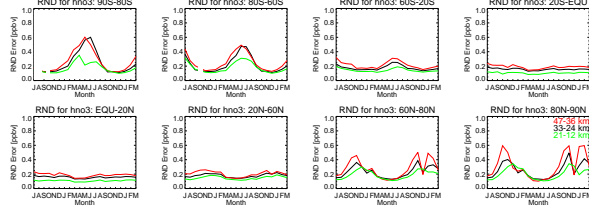


Figure 2. Time series of the random error derived from MIPAS Offline L2 data for HNO_3 [ppbv] from July 2002 to March 2004, for the same eight latitude bands.

All other target species present a similar behaviour with time. The predicted random error shows a distinct peak in the polar winter cases for the three height ranges in both hemispheres. The North polar winter shows a sharp dip in the middle of the peak probably corresponding to a stratospheric warming in December 2003.

The time variability of the predicted random error could be due to variations of the NESR (Noise Equivalent Spectral Radiance) with time, caused by the atmospheric variation of temperature.

Fig. 3 shows the time series of the NESR derived from MIPAS Offline L2 data for the period July 2002–March 2004 for the 5 different spectral bands. The NESR varies with time, steadily rising between decontamination events (shown by arrows in Fig. 3). The effect of this ice decontamination is a reduction of the gain increase and of the noise level [5].

Fig. 4 shows the time series of temperature. The temperature time series explains reasonably well the time series of the predicted random error for both hemispheres. The increase of random error at polar winters corresponds to decrease of temperature.

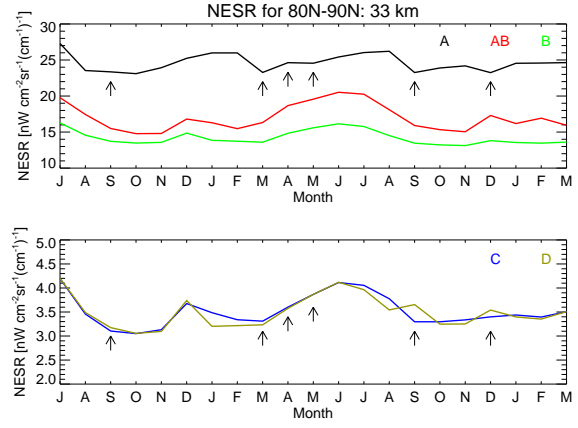


Figure 3. Time series of NESR derived from MIPAS LIB data for the 5 different spectral bands of MIPAS (A: 685–970 cm^{-1} , AB: 1020–1170 cm^{-1} , B: 1215–1500 cm^{-1} , C: 1570–1750 cm^{-1} , D: 1820–2410 cm^{-1}). Arrows show when ice decontamination occurred during the mission.

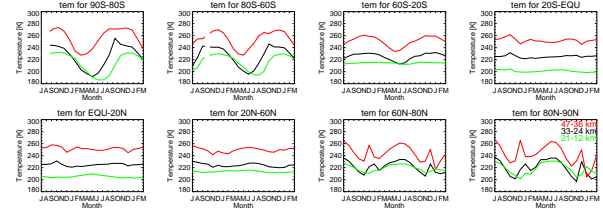


Figure 4. Time series of retrieved temperature [K] derived from MIPAS Offline L2 data.

3. PRECISION VALIDATION

The precision of the retrievals may be defined as the dispersion of an ensemble of retrievals obtained from limb measurements of the same atmospheric state. Although, in practice MIPAS does not make repeated measurements of the same limb path, an approximation is available from the pairs of measurements located at the intersections of the MIPAS viewing tracks. Therefore the precision of the retrievals can be estimated by examining these pairs of collocated measurements. Profile locations of ascending and descending tracks were matched to within 300 km in distance (compared to approximately 500 km distance between successive profiles along the orbit) for every 5 days per month of high resolution MIPAS operation. Limiting the comparisons of profile locations to 6 hours time difference and 300 km horizontal difference produces regular matches at two latitudes, near the poles, in the 80S–90S and 80N–90N regions. Extending the comparisons to 12 hours time difference produces matches at three additional latitudes in the regions 20S–60S, 60S–80S and 60N–80N. Fig. 5 shows the locations of the MIPAS profiles for 30 July 2003.

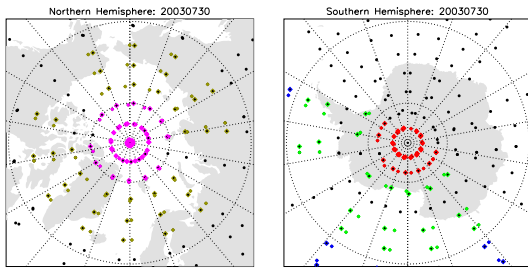


Figure 5. Locations of the L2 Offline ESA MIPAS profiles for 30 July 2003. Coloured points represent positions where orbital tangent tracks intersect when two observations are made of the same atmosphere 6 hours apart (red for S. Pole and magenta for N. Pole) and 12 hours apart (green, blue and yellow). The black orbit intersections in the South Pole regions come from observations made more than 12 hours apart.

In order to check the actual scatter of the measurements, where orbital tangent tracks intersect, the standard deviation of the ensemble of profile pairs is compared to the predicted random error given in the L2 data. The predicted random error takes also into account the pT error contribution for the species VMR.

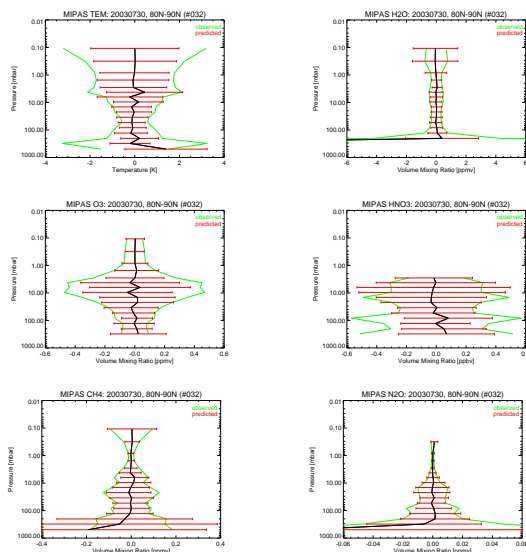


Figure 6. Example of polar summer comparisons at 80N-90N latitudes for 30 July 2003. It shows comparisons for temperature (top left), H_2O (top right) O_3 (middle left), HNO_3 (middle right), CH_4 (bottom left) and N_2O (bottom right). The black line is the bias between the matched pairs profiles, the red bars are the predicted scatter (for the VMR plots the pT error contribution is included) and the green line is the observed scatter.

Fig. 6 shows an example of the comparisons between the standard deviation of the ensemble of profile pairs and the estimated standard deviation given in the MIPAS data. This is a polar summer plot at 80N-90N latitudes

for 30 July 2003 for all target species but NO_2 since for NO_2 there is a large diurnal difference at the intersections of any two orbits.

In order to compare the time series of the observed scatter in the measurements with the predicted random error, the ratio of the statistic of observed scatter over the predicted random error was computed for the four latitudes bands and averaging over the whole profile of the target species. Fig. 7 presents the time series of the observed over the predicted scatter for each species for the July 2002 – March 2004 period. In this case the startospheric components of the profiles have been averaged up to the nominal tangent height of 15 km (after a filtering of profiles outside 100% of the mean latitudinal value). Even taking into account the propagation of the pressure-temperature retrieval errors into the VMR retrieval, the observed scatter is usually a factor 1-2 larger than the predicted error. For temperature, the ratio time series may be affected by the seasonal variation of atmospheric temperature for both polar regions since it increases in polar winters. In general the observed scatter for all species should be larger than the predicted since the standard deviation of the ensemble of profile pairs is an approximation of the random uncertainties and it includes the variability of the atmosphere. Moreover, it is thought to be due to the assumption of an horizontally homogeneous atmosphere in the retrieval.

REFERENCES

- [1] ESA, SP-1229: ESA ENVISAT-MIPAS: an instrument for atmospheric chemistry and climate research, European Space Agency, ESTEC, Noordwijk, The Netherlands, 2000.
- [2] Fischer, H. et al.: MIPAS: an instrument for atmospheric and climate research, Atmos. Chem. Phys. Discuss, in preparation, 2006.
- [3] Raspollini, P. et al.: MIPAS level 2 operational analysis, Atmos. Chem. Phys. Discuss, accepted, 2006.
- [4] Ridolfi, M. et al.: Optimised forward model and retrieval scheme for MIPAS near-real-time data processing, Appl. Opt., 39, No 8, 1323–1340, 2000.
- [5] Kleinert, A. et al.: MIPAS Level 1B algorithms overview: operational processing and characterization, Atmos. Chem. Phys. Discuss, under review, 2006.

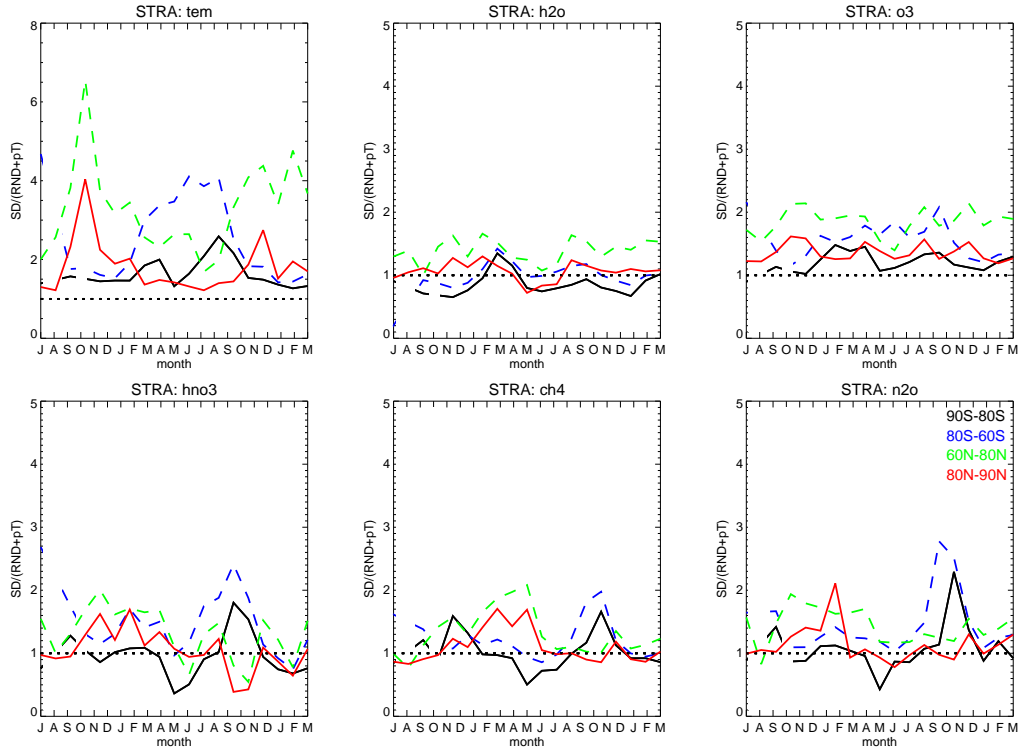


Figure 7. Time series of the ratio observed/predicted scatter for each species derived from the analysis of the matching ascending/descending profile pairs from July 2002 to March 2004. This ratio is computed averaging the whole observed/predicted scatter profiles up to the nominal tangent height of 15 km (stratosphere). For each species, Black indicates 80S–90S, Red 80N–90N, Blue 60S–80S and Green 60N–80N regions as a function of time. Solid lines indicate matching pairs within 6 hours, while dashed lines within 12 hours. The predicted scatter includes the predicted random error given in the MIPAS Offline L2 data and the pT error propagation component.

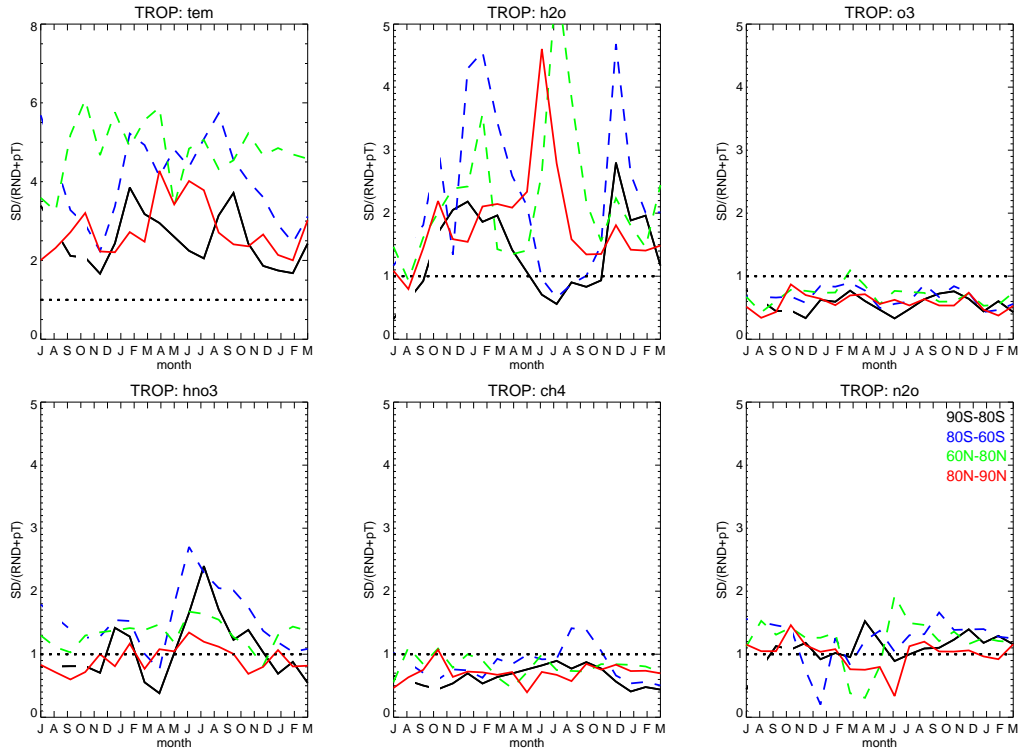


Figure 8. Same as Fig. 7 where instead of averaging over the whole profile up to the nominal tangent height of 15 km, the average is only over the lowest three nominal tangent heights from 6 to 12 km (i.e troposphere).